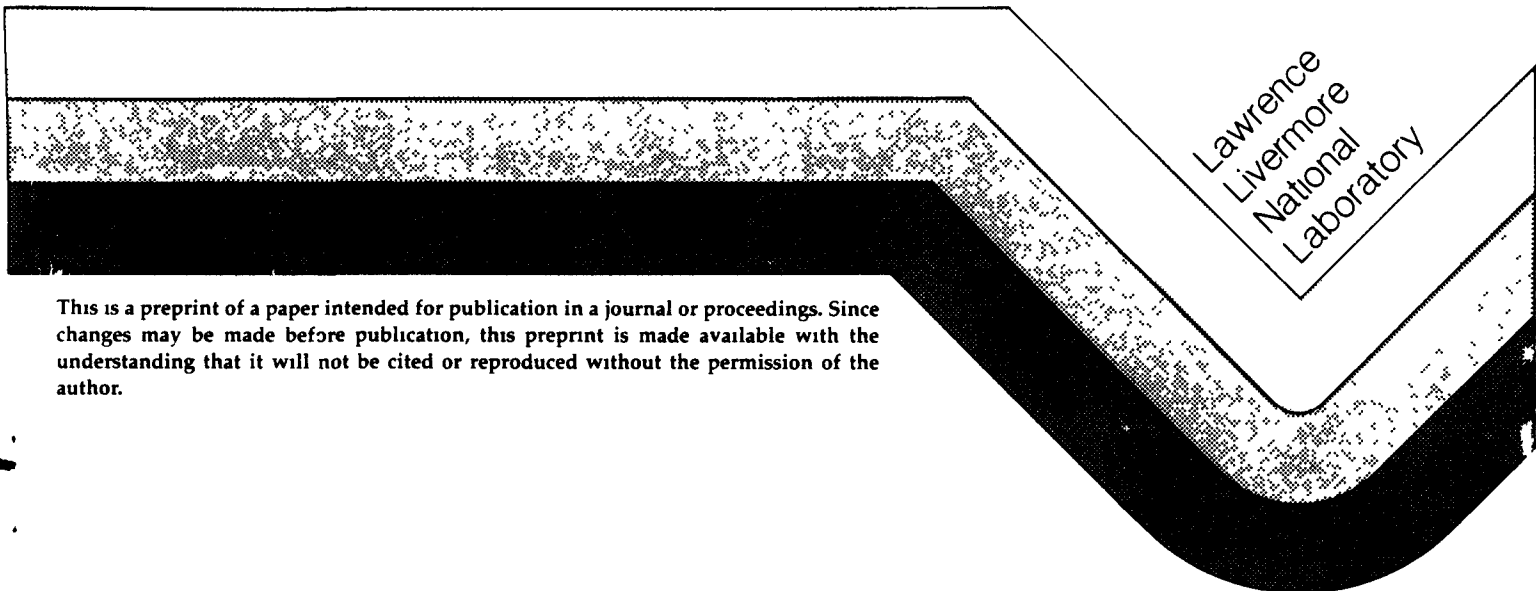


A D-T NEUTRON SOURCE FOR FUSION MATERIALS
AND TECHNOLOGY TESTING

F. H. Coengen
T. A. Casper
D. L. Correll
C. C. Damm
A. H. Futch
A. W. Molvik
R. H. Bulmer

This paper was prepared for submittal to the
Course/Workshop on Physics of Mirrors,
Reversed Field Pinches and Compact Tori,
Varenna, Italy
September 1-11, 1987

August 1, 1987



This is a preprint of a paper intended for publication in a journal or proceedings. Since changes may be made before publication, this preprint is made available with the understanding that it will not be cited or reproduced without the permission of the author.

DISCLAIMER

This report was prepared as an account of work sponsored by an agency of the United States Government. Neither the United States Government nor any agency thereof, nor any of their employees, makes any warranty, express or implied, or assumes any legal liability or responsibility for the accuracy, completeness, or usefulness of any information, apparatus, product, or process disclosed, or represents that its use would not infringe privately owned rights. Reference herein to any specific commercial product, process, or service by trade name, trademark, manufacturer, or otherwise does not necessarily constitute or imply its endorsement, recommendation, or favoring by the United States Government or any agency thereof. The views and opinions of authors expressed herein do not necessarily state or reflect those of the United States Government or any agency thereof.

DISCLAIMER

Portions of this document may be illegible in electronic image products. Images are produced from the best available original document.

A D-T Neutron Source for Fusion Materials and Technology Testing

F.H. Coengen, T.A. Casper, D.L. Correll, C.C. Damm,
A.H. Futch, A.W. Molvik, and R.H. Bulmer
Lawrence Livermore National Laboratory, University of California,
Livermore, CA 94550, U.S.A.

1 Introduction

This report describes a conceptual design of a high-fluence source of 14 *MeV* D-T neutrons for accelerated testing of materials. The design goal of 10 *MW/m²* year corresponding to 100 displacements per atom per year is taken to be sufficient for end-of-life tests of candidate materials for a fusion reactor. Such a neutron source would meet a need in the program to develop commercial fusion power that is not yet addressed. In our evaluation, a fusion-based source is preferred for this application over non-fusion, accelerator-type sources such as FMIT because, first, a relevant 14 *MeV* D-T neutron spectrum is obtained. Second, a fusion source will better simulate the reactor environment where materials can be subjected to high thermal loads, energetic particle irradiation, high mechanical stresses, intense magnetic fields and high magnetic field gradients as well as a 14 *MeV* neutron flux of several *MW/m²*. Although the actual reactor environment can be realized only in a reactor, a fusion-based neutron source can give valuable design information of synergistic effects in this complex environment.

The small-volume, high-fluence source we are proposing would complement the capabilities of a facility such as ITER, which addresses toroidal fusion component development. High-fluence operation of the latter facility would be difficult, expensive, and wasteful since only relatively small test volumes are necessary for materials evaluation. For our source, the volume of reacting plasma and the fusion power have been minimized, while maintaining an intense neutron flux. As a consequence, tritium consumption is modest, and the amount of tritium required is readily available.

In our preliminary study, we have not specifically addressed costs for the proposed facility. The major cost item, however, is certainly the power drive system, both in capital investment and operating cost. We have endeavored to minimize the beam power required and have calculated suitable parameter regimes at a beam power of ~ 50 MW. This is a substantial, but perhaps manageable level and leads us to think of a capital and operating budget competitive with FMIT. Capital costs would certainly be well under the levels expected for ITER, so we can legitimately consider such a source as an adjunct to the main fusion development program. Furthermore, as will be seen in later sections of this report, an optimum beam energy for the neutron source is in the range of 200 – 250 keV. This is somewhat less than the value anticipated for ITER beams, but we expect that a common development program would provide beams for the neutron facility at minimal additional cost. With beam power requirements in the 50 MW range, there is also the possibility of sharing the actual power supplies between the ITER and neutron source facilities.

In approaching a design for a compact, intense neutron source, we focused on a linear two-component plasma system [1]. To minimize power loss at the ends, we have considered magnetically restricted flow regimes, involving either a simple high-field mirror system or a multiple-mirror regime. For various reasons involving either the performance obtainable at reasonable technology levels, or the uncertainties involved in the physics extrapolation, we have rejected these approaches to restricting the power flow in favor of that described in the next sections.

2 Neutron Source Concept

In our design D-T neutrons are produced in a linear, two-component plasma formed by neutral beam irradiation of a fully ionized warm plasma target. The usual problems associated with deposition of high-power densities in a solid target have been avoided through the use of a fully ionized plasma target that is sufficiently dense to stop all of the energetic beam particles and that is hot enough ($T_e \simeq 200$ eV) to significantly increase the D-T reaction rate above that obtained with solid targets. The beam energy deposited in the center flows along the target plasma column to end regions where it is absorbed in neutral gas at high pressure. A distinctive feature of our approach is that the target plasma is operated in a regime where electron thermal conduction along the column is the controlling energy-loss process.

The loss rate can be minimized by adjustment of the diameter and length of the plasma column. Furthermore, a substantial gradient in T_e along the column results in considerable recombination of the plasma to gas in the end regions before impact on the end walls.

The resultant hot gas is cooled by contact with large-area heat exchangers. In this way, the large steady-state heat load from the injected neutral beams is diffused and removed at tolerable heat flux levels. A similar approach to handling large heat loads has been proposed in relation to tokamak divertor design, and an experimental simulation of a gaseous tokamak divertor was described by W. Hsu *et al.* [2] in 1982. In that experiment, the plasma was cooled and absorbed in a gaseous end region, much as we propose.

The basic elements of the neutron source design are shown schematically in Figure 1. There are three well-defined plasma regions: the central neutron production region, a power transport region, and a gas-heat exchange region.

In the central region, high-energy neutral beams of deuterium atoms are ionized in the warm, dense tritium target plasma with the resulting hot deuterons trapped in a quadrupole-mirror field.¹ As the deuterons slow down by collisions with the target electrons, they interact with the tritium to generate the desired D-T fusion neutron flux. At electron densities of the order of 10^{15} cm^{-3} , the characteristic loss time of hot ion energy to the cold electron population (τ_{drag}) is $\sim 100 \mu\text{s}$ and is much shorter than the ion scattering time (τ_s). Consequently, the hot ion density remains localized in the center, requiring only a low mirror-ratio quadrupole for confinement. This central minimum-B region of high P_{\perp} provides the necessary MHD stability for the entire device since plasma pressures are low elsewhere. The localized, non-Maxwellian hot-ion component, however, provides an opportunity for microinstability. Microstability, plasma equilibrium, MHD stability, and β -limits are important questions that will be addressed in later sections of this report.

The trapped deuterons in the central region degrade in energy to the point where nuclear interaction becomes improbable; they continue to cool until they join the warm target population and eventually diffuse out the ends of the device. The heated electrons share their energy by frequent collisions with target ions, so $T_i \approx T_e$ in the warm plasma.

¹While we specify a quadrupole to be definite, we do not rule out the possibility of axisymmetric stabilization, for instance by a "divertor" coil as tested on TARA. Coil simplicity and improved access would be worthwhile improvements provided performance, i.e., β -limits, could be maintained.

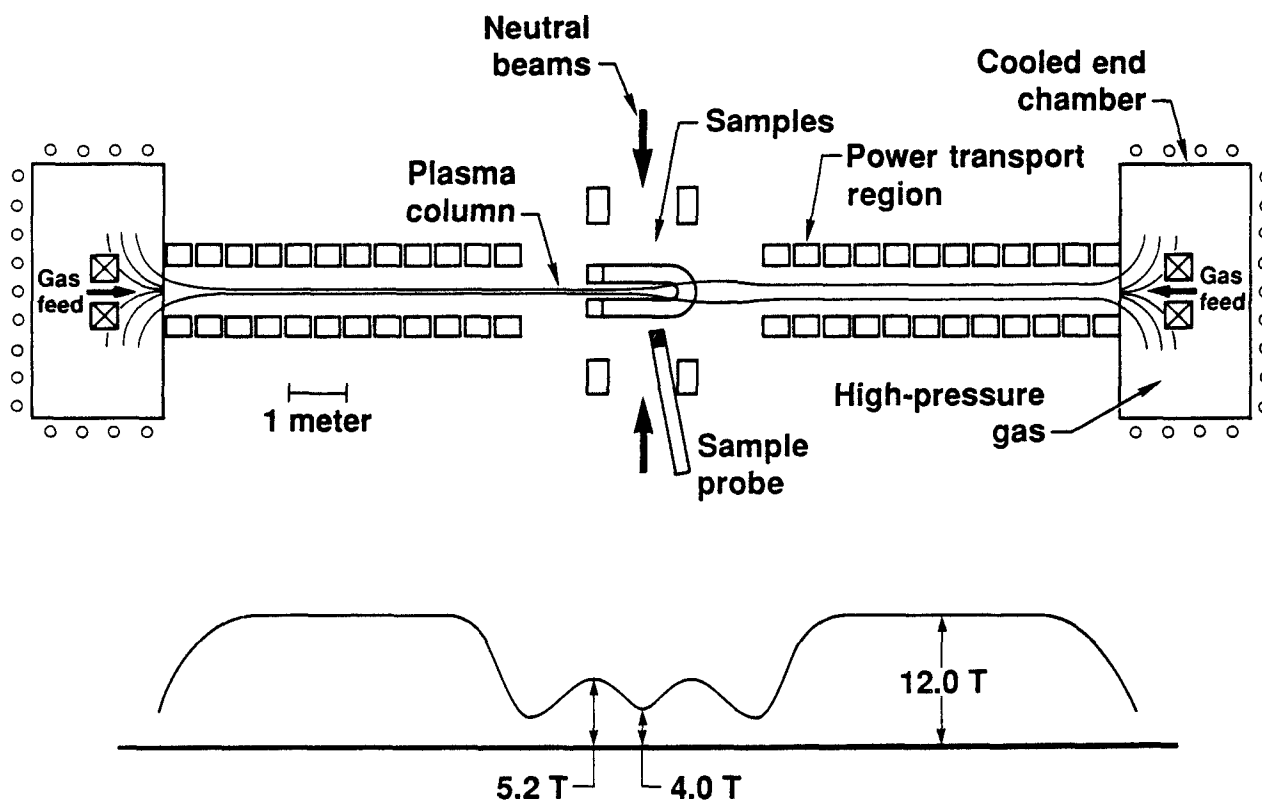


Figure 1: Schematic of the high-fluence neutron source.

In the power transport region, the target plasma is collisional so conduction losses from the center are reduced by the ratio of the magnetic field (hence area) at the center to that in the transport section. The maximum practical field is used in the transport region to minimize the conduction. Power is further reduced by lengthening this section.

In developing our conceptual design, we have assumed one-dimensional power and particle flow in the direction of the magnetic field. In steady state, local values of density and temperature are assumed to remain constant and the pressure (nkT) is assumed constant throughout the system. Thus, in effect, the longitudinal plasma pressure at the center is balanced by the neutral gas pressure of order one atmosphere in the end chamber. There is a net particle flow equal to the neutral particle injection rate from the center to the end chambers where gas is removed, or added, as necessary to maintain a constant pressure in these tanks.

In the end regions, the now cold, dense plasma is flared to a thin cross section so that interaction with the ambient gas can result in recombination before striking the end walls. The hot gas is finally cooled either by radiation and convection to the large-area walls or by circulation through large-area heat exchangers.

The gas in the end regions also serves to fuel the warm tritium plasma. Details of how this is accomplished to maintain the steady-state density distribution remain to be worked out but will probably involve a differential pumping system to adjust gas flows.

3 Plasma Modeling and Parameter Study

3.1 General Constraints

The desired neutron flux of 5–10 MW/m^2 is achieved at minimum beam power by adjusting the many parameters of the device to an optimum combination that is consistent with technological and physics constraints. In setting the parameters, our goal is to minimize extrapolation of well-established physics and to keep the technological requirements to the level of existing capability, or at most, to the level of development needed for ITER.

First, it can be readily demonstrated that, for given magnetic field and plasma β , the maximum reaction rate (hence neutron flux) is realized in the two-component mode with one hot species and one warm species of equal density. If β limits the hot density to a lower value, the warm density

can be increased to reach a total density determined by beam penetration requirements (see below). [The conditions for maximum neutron production will not, of course, result in maximum Q .] The volume of reacting plasma is minimized by limiting the length to the size of the neutral beam, and the diameter to $\sim 6 \bar{\rho}_i$, or approximately 3 average ion gyro-orbit diameters. For practical central magnetic field intensities of $\sim 4 T$, this diameter restriction will require a well-focused neutral beam. As will be discussed, the resulting dimensions appear to be compatible with the test-volume requirements for a materials test program.

A central minimum-B type magnetic field of $4 T$, mirror ratio 1.2, can be generated using superconducting circular coils in combination with a quadrupole copper insert, as indicated in Fig. 1 and discussed in Appendix A. The copper insert need not be shielded from the neutrons but does require significant drive power. The advantage of a low-mirror-ratio requirement becomes apparent here.

To minimize the heat flow along the plasma column, the column diameter is minimized by using the maximum practical intensity for the guide field. Superconducting solenoids of suitable diameter have been tested to $12 T$, and we use this value for our solenoidal guide field. The length of the guide field was selected as $5 m$ (each end) from a parameter study (see Sec. 3.3) that showed diminishing improvement beyond this length.

A constraint on total plasma density is set by the requirement that the neutral beams penetrate to the axis. We have chosen the product of density and plasma radius to equal two mean free paths for beam trapping, $na = 2\lambda_{trap}$. With this choice, a substantial fraction of the beam does penetrate to the axis, but is almost completely absorbed before leaving the target. The beam-trapping estimate includes a correction for multistep collision processes that increase trapping rates [10].

The hot component of the plasma essentially determines the plasma pressure. Our parameter study, not unexpectedly, shows improved performance as a function of increasing β , with values of β in the range of 0.4 to 0.6 required if beam power is to be held to the level of $\sim 50 MW$. In our modeling calculations (Sec. 3.3), we determine β and beam power in relation to neutron flux. A limiting value for β set by equilibrium and MHD stability remains as one of the important physics issues (Sec. 4).

3.2 Plasma Modeling

The power flow from the central plasma to the ends is based on Spitzer [3] conductivity:

$$P_{cond} = 2K \frac{\delta T_e}{\delta Z} A, \text{ with } K = 29.4 T_e^{5/2} (\text{eV}) = \frac{4\pi a^2}{l_c} \int K D - T_e (W) \quad (1)$$

In this expression, l_c is the full length of the plasma column and a is the radius. The theory only applies for $\lambda < l_c/2$, where λ is the electron-electron mean free path,

$$\lambda = \frac{2 \times 10^{13} T_e^2 (\text{eV})}{n_e \ln \Lambda}. \quad (2)$$

The condition $\lambda < 500 \text{ cm}$ is shown in Fig. 2; below the dashed lines, the n_e and T_e values support a Spitzer conductivity model for electron power balance. Above the line, i.e., $\lambda > l_c/2$, collisionless power flow due to thermal convection is the proper model. Under these conditions, sheath potentials develop to lower the electron particle flux to ensure that the electron heat flux remains below $n_e v_e T_e$. A more complete treatment of axial power loss concerning both regions is discussed in Ref. [11]. The nominal operating point for our present neutron source is shown to lie well within the Spitzer conductivity region (Fig. 2). Some confidence in the thermal conduction model is obtained from high-energy θ -pinch experiments [4].

Assuming the power loss to be by thermal conduction, we can equate this to the power input to the plasma through electron drag of injected deuterons:

$$P_{drag} = V \frac{n_h n_e \bar{E}_h e}{(n\tau)_{drag}}, \quad (3)$$

where $V =$ hot plasma volume, assumed cylindrical;

$n_e =$ total density;

$n_h =$ hot density;

$\bar{E}_h =$ average hot ion energy;

$e =$ electronic charge;

$$(n\tau)_{drag} = 1 \times 10^{13} A_i T_e^{3/2} \frac{1}{\ln \Lambda}.$$

Therefore, for deuterons, where $\ln \Lambda = 11.6$, $(n\tau)_{drag} = 1.73 \times 10^{12} T_e^{3/2} (\text{keV})$.

Equating $P_{cond} = P_{drag}$, we obtain an expression for T_e :

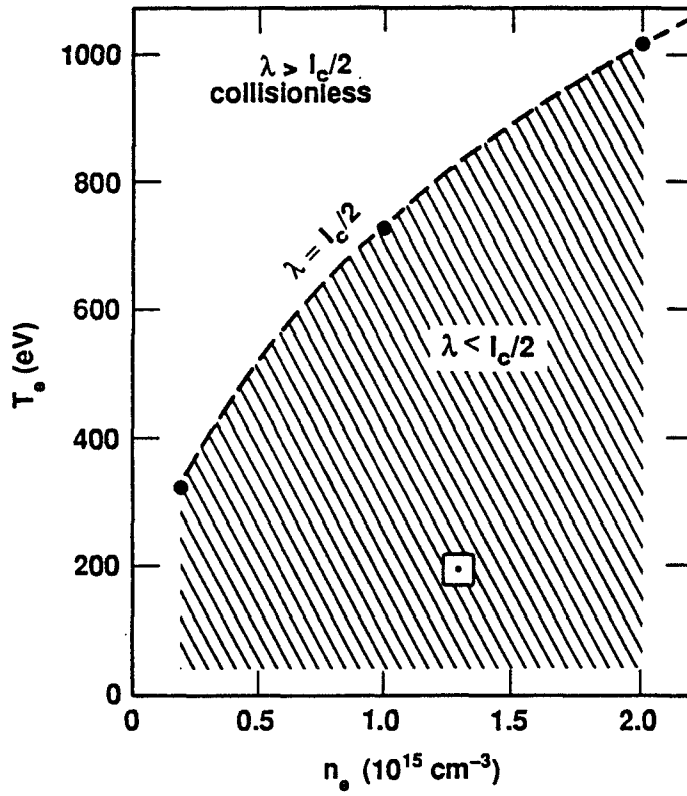


Figure 2: Electron temperature limits defining a region where the thermal conduction modeling applies, i.e., $\lambda < l_c/2$. The data point denotes our nominal operating point.

$$T_e(\text{keV}) = 9.72 \times 10^{-9} (n_h \bar{E}_h n_e l_h l_c R)^{1/5}, \quad (4)$$

where l_h = length of hot plasma, and R = ratio of field in solenoid to central field.

The hot ion density is calculated from a maximum value of β estimated for the mirror mode instability unless this value of n_h is greater than one-half the total density, ($n_e/2$). If the limiting n_h is greater than $n_e/2$, then n_h is set equal to $n_e/2$ to maximize the reaction rate.

The neutron flux Γ is calculated from a flat-profile, cylindrical model and is quoted at the plasma surface of radius a . Corrections for finite plasma length and for a wall at radius r_w will result in a decrease in useable neutron flux. The flux is calculated from the formula:

$$\Gamma = n_w n_h (\bar{\sigma} \bar{v}) E_f (\text{eV}) / S \quad (5)$$

where E_f is the neutron fusion energy released per reaction, n_w is the density of the tritium target, V is the hot plasma volume, and S the hot plasma surface area. For a cylindrical plasma of radius a with parameters expressed in *cgs* units,

$$\Gamma = 1.12 \times 10^{-14} n_w n_h (\bar{\sigma} \bar{v}) a (\text{MW}/\text{m}^2) \quad (6)$$

For our parametric scaling studies, a midplane magnetic field of 4 T was chosen such that for the optimum injection energy ($\sim 200 \text{ keV}$), a plasma having a radius of approximately $3 \bar{\rho}_i$ would correspond to the anticipated dimension of a well-focused neutral beam. The average gyro-radius $\bar{\rho}$ for the hot deuterium ions was determined from the average hot ion energy.

For use in our analytic model, we have used plasma parameters based on square-well Fokker-Planck calculations of the hot ion distribution function at the midplane. The multi-species Hybrid II code [5] was used for the calculation of the hot ion distribution junction and average values for $(\bar{\sigma} \bar{v})$ D-T and the hot ion energy, \bar{E}_h .

Since the hot ion drag time is much faster than the ion-ion scattering time, the hot ions are confined to the central cell with negligible pressure weighting in the non-minimum B sections of the magnetic field. This assures the MHD stability of the plasma. We have also modeled the plasma with the Z-dependent SMOKE code [6] to verify this conclusion.

In the Fokker-Planck calculations, T_e is an input parameter so it is necessary to iterate between the analytic expression for T_e and the code to obtain a consistent set of values for T_e , \bar{E}_h , and the other related variables.

Assuming the hot ion distribution to be fixed by neutral beam injection in the central location, we also investigated the formation of self-consistent axial density and temperature profiles using the PHLOW code [12] with the addition of the axial conduction model. The code solves the warm ion fluid equations with sources to determine the interaction of the tritium neutrals injected at an axial location of 700 *cm*. The hot ions were modeled as a fixed species with an average energy of 50 *keV*, a peak density of $0.4 \times 10^{15} \text{ cm}^{-3}$, and a length of 60 *cm*. The resulting equilibrium axial profiles are shown in Fig. 3. The important features are an achievable operating condition with $n_{ci} \simeq 0.5 \times 10^{15} \text{ cm}^{-3} \simeq n_{hi}$ at a central electron temperature of 250 *eV*. These results are consistent with the analytical model presented earlier. We also note the cold ions remain Maxwellian with $T_{\perp} \simeq T_{\parallel}$ over the length of the device. The electron temperature is observed to decrease along the axis with a more precipitous drop at the location of the tritium gas source. The achieved operating condition required the injection of 1,200 *A/cm*² of gas evaluated at the midplane (or roughly 60,000 *A* of neutral gas for a 5 *cm* radius plasma). This corresponds with a total power requirement of about 18 *MW*. These preliminary calculations indicate that the desired fueling technique and operation appear feasible.

3.3 Results of Modeling Calculations

To determine a length for the solenoidal power transfer region, we have calculated neutron flux and power versus total length, l_c , of the plasma column. These estimates were done for $B_0 = 5 \text{ T}$, at three values of injection energy. Flux levels are predictably flat with l_c , Fig. 4, with a good indication, however, of the advantage of $\sim 200 \text{ keV}$ injection. Power decreases with l_c but the gain beyond $l_c \sim 10 \text{ m}$ (5 *m* each side of center) is small. For our present purposes, we chose $l_c = 10 \text{ m}$ as our standard length in all that follows.

Selection of an optimum beam energy is not clear-cut without additional constraints. At low injection energies, average deuteron energies are low and the reduced D-T reaction rates result in a high β value if significant neutron flux is to be realized. At high beam energies, reaction rates are improved but the larger ion gyro-diameter forces plasma size to increase, raising the power requirements substantially. One approach to selecting an optimum beam energy is shown in Fig. 5.

Here we plot beam power and β vs beam energy for a fixed value of $\Gamma = 8 \text{ MW/m}^2$. If β must be less than some limit (for example, 0.6) and beam power is limited somewhat arbitrarily (to say, 50 *MW*), then beam

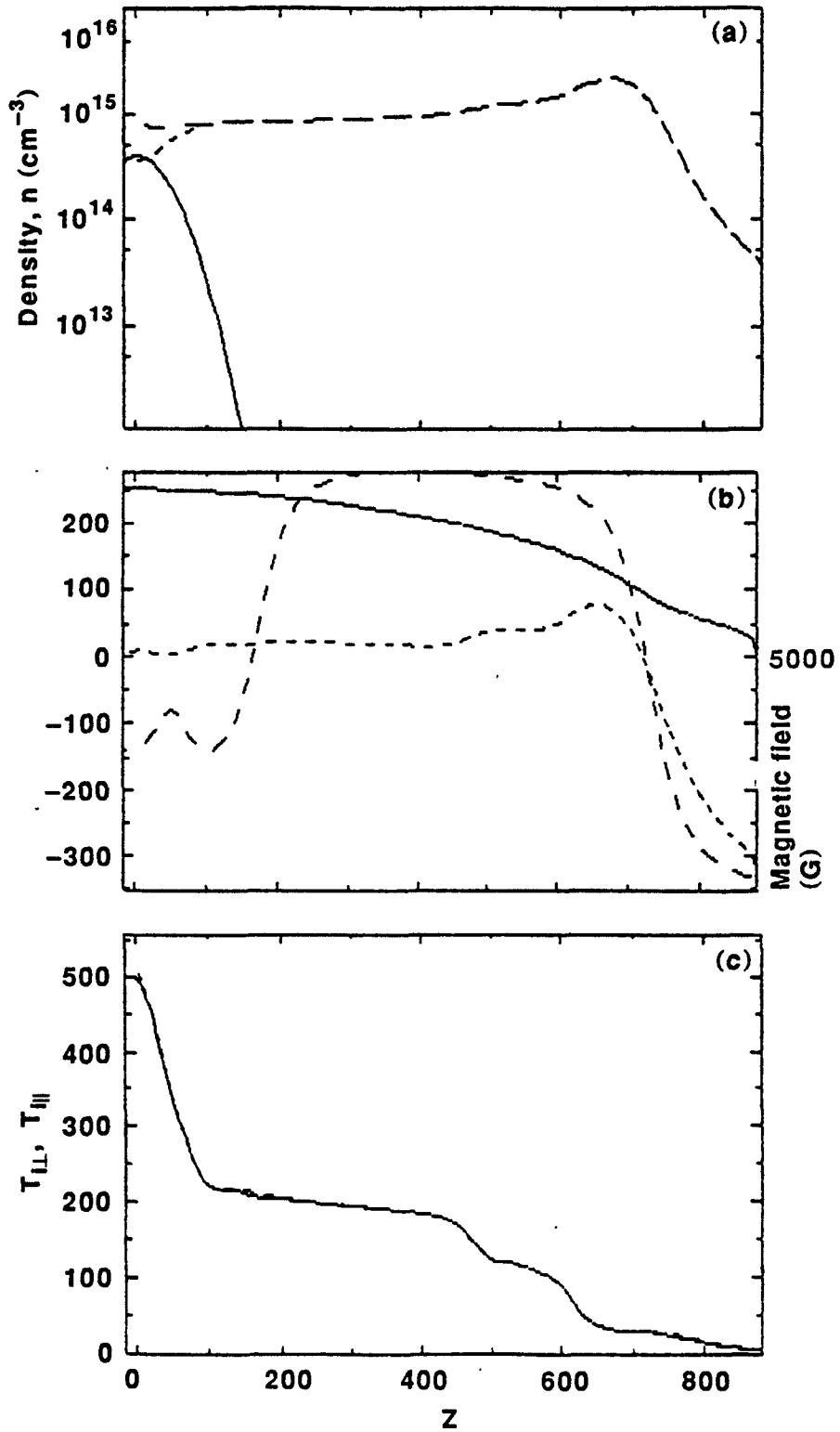


Figure 3: PHLOW code results for a fixed hot deuterium plasma at $n_h = 0.4 \times 10^{15}$ and $E = 50 \text{ keV}$: (a) ion density profiles for hot (—) and cold (---) species; (b) axial profiles of electron temperature (—), potential (---), and magnetic field (- · -); (c) cold ion $T_{i\perp}$ and $T_{i\parallel}$ indicating an isotropic cold species.

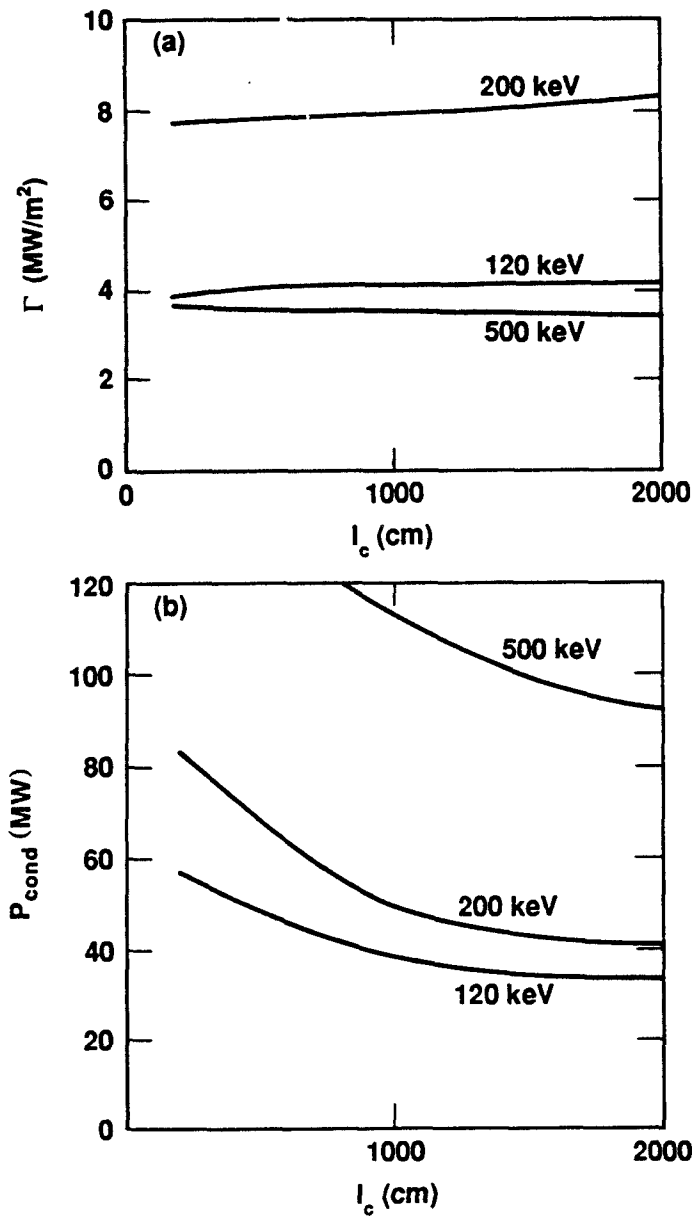


Figure 4: Variation of power and neutron flux, Γ , with total column length, l_c , for three values of D° injection energy.

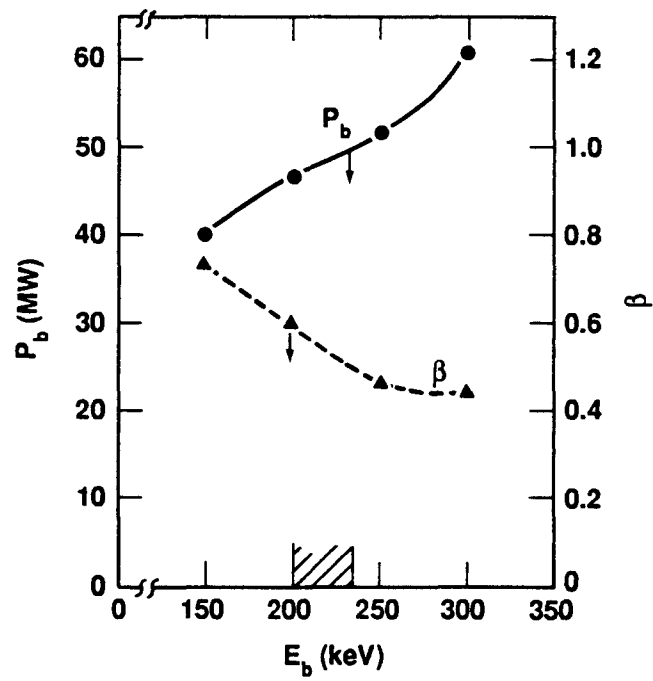


Figure 5: Beam power, P_b , and β vs beam energy, E_b , at constant $\Gamma = 8 \text{ MW/m}^2$. If $P_b \leq 50 \text{ MW}$ and $\beta \leq 0.6$, then E_b must lie between 200 and 235 keV.

energy must be in the range of 200–240 keV.

In an early study of two-component plasmas, Hiskes *et al.* [7] also find injection at ~ 200 keV to be optimum. Also, current studies of an intense neutron source by Ryutov and Mirnov [8] in the USSR set the optimum injection energy at 240 keV. For our present purposes, we select 200 keV as a “base case” injection energy. If technological or economic considerations set the beam energy at either higher or lower values, it should be noted that interesting neutron fluxes could still be realized. A beam energy of about 150 keV, for instance, might allow use of positive-ion beam technology with substantial savings in beam development. Alternatively, beam development for ITER could provide the necessary technology for a more optimum source beam energy at minimum additional cost.

Selection of $B_0 = 4$ T for the central field intensity is based on meeting practical requirements for the copper quadrupole insert, in terms of beam access and magnet drive power. Fig. 6 shows improved performance in terms of Γ as B_0 is increased although the improvement is less dramatic if Γ is specified at a fixed wall radius (6 cm). More refined trade-off studies will eventually be required to set B_0 . In Fig. 7, we have plotted the neutron flux, Γ , and plasma β vs injected beam power for our nominal “base case,” with 200 keV beam injection and $B_0 = 4$ T. Table 1 lists plasma parameters at an operating point with $\beta = 0.6$.

We have estimated heat loads resulting from charge-exchange processes for the base case parameters. Including exchange with both beam and gas, total heat loads on a wall at $r = 7.5$ cm are less than 180 W/cm² and can be handled with conventional cooling. Also, α -particle loads on end plates (central region) are estimated at less than 125 W/cm² and can be readily removed.

The “base case” dimensions of the reacting plasma are 7.5 cm diameter and 30 cm length. Access for materials test probes is adequate to provide test volumes at least as large as those specified for the FMIT (see the FINESSE report [9]). We therefore anticipate that the proposed source will be suitable for the intended application.

3.4 Possible Refinements to Modeling

Several factors not yet adequately included in our plasma modeling can influence estimates of performance. On the positive side, one could take advantage of finite orbit effects, using offset beams to overcome limitations on density imposed by the beam trapping. We can imagine gains of factors

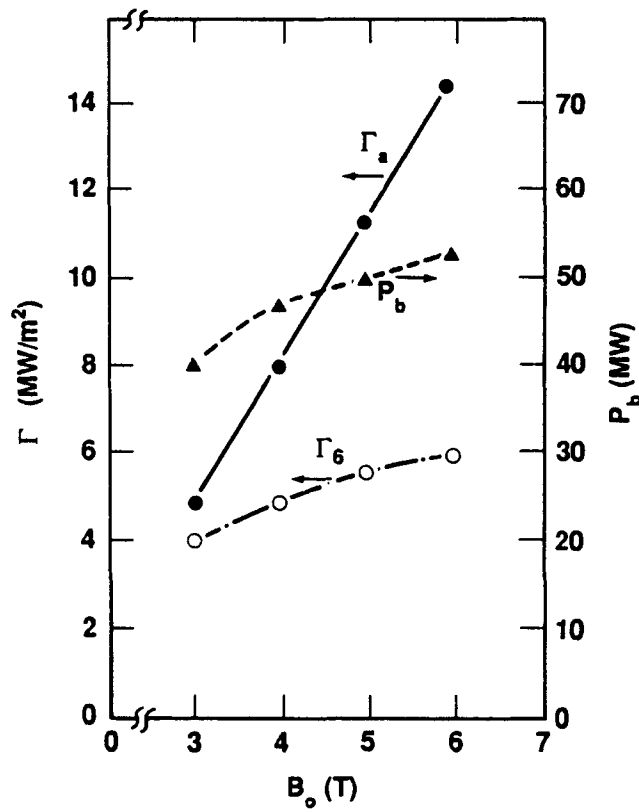


Figure 6: Neutron flux, Γ , and beam power, P_b , as a function of central field intensity, B_0 . Γ_a is measured at the plasma surface, Γ_6 , at a radius of 6 cm.

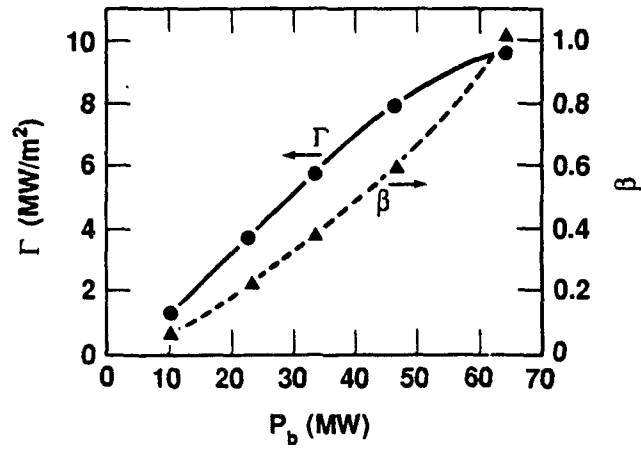


Figure 7: Neutron flux, Γ , and plasma β vs beam power, P_b , for “base case” parameters: 200 keV D^0 beam injection, $B_0 = 4 T$, plasma radius $a = 3.75 cm$.

Table 1: Nominal Operating Point Parameters

| | |
|-------------------------|--------------------------------------|
| D° beam energy | 200 keV |
| D° beam power | 47 MW |
| Neutron flux, Γ | 7.9 WM/m ² |
| Total fusion power | 0.7 MW |
| Plasma β | 0.6 |
| n_h | $3.9 \times 10^{14} \text{ cm}^{-3}$ |
| n_e | $1.3 \times 10^{15} \text{ cm}^{-3}$ |
| T_e | 190 eV |
| \bar{E}_h | 63 keV |
| l_h | 30 cm |
| a | 3.75 cm |
| $\bar{\rho}_i$ | 1.24 cm |
| l_c | 10 m |
| B_0 | 4 T |
| B_M | 12 T |
| Quadrupole magnet power | 6.8 MW |

of 2 in neutron flux by this technique. A smaller gain of perhaps several percent is expected from a more detailed evaluation of $(n\tau)_{drag}$, arising from a correction when, as in our case, $\bar{v}_i \gtrsim v_e$.

On the negative side, the cylindrical approximation used for estimating Γ gives too high a value by perhaps 25%. It is also not clear how close to the nominal plasma surface samples can be placed. At larger radii neutron flux is, of course, lower.

A third factor reducing the estimated neutron flux is the density of deuterons in the warm plasma due to degraded ions that are in the process of diffusing out the ends of the device. Preliminary estimates of this effect have been obtained by a simplified Monte Carlo calculation [13] of the hot ion component diffusion in energy in a fixed warm tritium background. Estimates of this deuterium "contamination" are in the range of 5-10 % of the tritium density; therefore, this appears not to be a serious problem. More detailed Monte Carlo calculations are planned.

Finally, we note that there is some indication from θ -pinch [4] that thermal conduction is higher than the theoretical value we have used by a factor of 2-3. This is a serious correction if it applies in our case.

4 Physics Issues

The main physics issues affecting neutron source operation which must be addressed include:

1. Steady-state fueling of the hot ion species from the end region to achieve densities in excess of $1 \times 10^{15} \text{ cm}^{-3}$.
2. The ability to self-consistently control the heat conduction consistent with the end-fan fueling requirements.
3. β -limits based on equilibrium and MHD stability constraints in the minimum-B region.
4. Ion microstability of the MHD stable high beta plasma and the amount of additional cold ion heating (added power loss) that results to satisfy instability demands.

These issues can be addressed in a smaller scaling experiment to improve the existing physics data base and to determine the range of validity of the existing theory. This will provide us with the ability to more accurately predict neutron source operation.

In our preliminary analysis and design, we have implicitly assumed that the power flow is determined solely by electron conduction in the strongly collisional regime. The power flow from the neutral beam-driven hot ion component to the lower energy ion end losses must be dissipated in the end fan region by the high-pressure gas consistent with the required fueling rate. While there is experimental justification for the heat conduction model used based on θ -pinch [4] experiments, verification of the limits of applicability and the interaction with the streaming neutral gas are required. We are beginning to investigate the axial variation of the ion and electron temperatures with a Monte Carlo code to obtain the expected fueling and power flow conditions. The experimental issues of concern are the spatial variation of the actual power flow during operation where the fluid ion flow stagnates and our ability to independently control the power deposition and ionization processes required to achieve the desired fueling rate. These issues determine the length of the uniform high-field solenoidal region, the end wall materials and cooling requirements, and the technique for fueling in the end region. Considerable advantages may be achieved by properly tailoring the end regions of the device depending on the heat load and fueling requirements.

Since the economics of operation is mostly determined by the efficient use of the magnetic fields, we wish to drive the system at the highest plasma pressures possible, that is, at maximum beta. Our anticipated operational values for beta lie in the range of 0.4 to 0.8 and are thus in the range of equilibrium and MHD stability limits. The 2XIIB single mirror experiment previously operated routinely in the 0.4 to 0.6 range and under field reversal neutral beam injection aiming at values of peak beta in excess of 1 [14]. While the existing theoretical tools have failed to predict some of the higher beta values observed in 2XIIB, they do indicate the possibility of performance with beta in the range of 0.4 before equilibrium and MHD stability limits in the minimum-B configuration are encountered. We thus feel confident that we will be able to achieve reasonably good performance in such a neutron source. However, in order to understand the experimentally observed high betas relative to the code predictions and thereby be able to predict enhanced performance and scaling of operation, we must determine the existence and nature of the true beta limits.

Although we have satisfied the equilibrium and stability requirements for high beta operation, our desired level of performance is still not guaranteed since the mirror-confined ion velocity distribution must satisfy certain microstability requirements. Ion microinstabilities such as the drift cyclotron loss cone (DCLC) and Alfvén ion cyclotron (AIC) modes have been observed to degrade confinement in many earlier mirror experiments. For operation of a neutron source in the two-component mode, we expect that the DCLC modes will be stabilized by the large cold ion component in much the same manner as was observed in the Tandem Mirror Experiment (TMX) end cells. This assumes that the cold component is sufficiently warm so as to avoid a two-component type of instability. The growth rate of the AIC mode was limited in the TMX experiment (which employed perpendicular neutral beam injection) by cyclotron damping on the cold ion component with a resultant heating of the end loss species. This effect can be expected to enhance stability to the DCLC mode by increasing the cold temperature to better match the velocity space hole. This leaves AIC as the microinstability of most concern. The net effect of limiting the AIC growth rate by heating the cold ions to dilute the velocity space anisotropy is that we may need additional neutral beam injection to supply the power lost to the cold background to meet these AIC stability requirements. This additional injection power will be minimized somewhat by the amount of trapping of the cold species in the 3:1 mirror ratio of the high field solenoids. We are presently utilizing a Fokker-Planck code to study the ion velocity distribution resulting

from classical processes. These will be used with the various stability codes to determine the microstability requirements for the resulting distribution. The Fokker-Planck, stability, and Monte Carlo calculations will be used to determine a self-consistent operating condition for the neutron source with verification of these results obtained from the smaller scaling experiment.

5 Experiments to Address Physics Issues

Prior to completing a final design of the proposed neutron source, it will be necessary to establish a firm, quantitative basis for all of the physics assumptions involved in the concept. The mission of this facility does not involve any test of plasma physics, and the substantial cost of the facility precludes any chance for error in the basic design. Consequently, we envisage a set of modest test experiments to establish the necessary design data, followed by a scaling experiment that simulates full-level plasma operation, but without tritium. The fact that our concept does not involve any large departure from known physics leads us to believe that such a set of experiments can clearly provide the basis for final design.

The first tests we anticipate relate to β -limits, as suggested in Sec. 4. Somewhat surprisingly, there has never been a systematic test of MHD limits in minimum-B geometry. The most relevant measurements are those made in the 2XIIB experiment in 1975. Values of β in the range of 0.7 – 1.0 were measured, without any apparent limiting instability. For reasons not yet understood, theoretical estimates of β -limits for this experiment tend to be significantly lower than the experimental values. We are currently attempting to improve the theoretical estimates. However, we believe that it will be necessary to verify our theoretical extrapolations with an experimental study of MHD limits, systematically varying mirror ratio and well depth to test stability over a β range from ~ 0.1 to 0.5 or higher. A first look indicates this could be accomplished using magnets and neutral beams from TMX with a minimum amount of new gear and adaptation. We are in the process of designing this experiment.

In the same set of experiments, we anticipate additional data relating to microstability, in particular to the AIC mode most in question (Sec. 4). Data from 2XIIB, TMX, and TMX-U, and a good theoretical understanding of the mode should provide sufficient information to proceed with a final scale-up test.

As a second phase of the modest test experiment devised for MHD tests,

we envisage adding a warm plasma column to quantitatively test our ideas on heat conduction, fueling, plasma cooling, and absorption in the end regions. Estimates indicate this could be done with available 20 keV neutral beam power, reaching central electron temperatures of 40 – 50 eV for an adequate first test. This phase of our experimental series is not yet as fully developed as the MHD-test phase.

While we anticipate that a successful set of modest experiments as described above would give us a sufficient basis for design of the neutron source, prudence dictates a scale-up test, without tritium. To minimize the cost of a scale-up, we could compromise on items such as full steady-state operation, beam energy, and magnetic field strengths. Utilization of MFTF components is a possibility. The objective would be to test the complete configuration with parameters as close to final values as possible, allowing deviations where the required extrapolation will be beyond any doubt.

Appendix A. Magnet Design

We have completed a preliminary layout of magnets to match the requirements of our neutron source parameters. All solenoidal magnets Fig. A1, are specified as superconducting, and sufficient clearance has been introduced to allow for neutron shielding. The quadrupole insert is of copper and is meant to operate without shielding. Enlarged views of the central region are shown in Figs. A2 and A3, with attached scales to show dimensions.

The axial field plot is shown in Fig. A4. A central field of 4 T and a solenoidal field of 12 T meet our parameter specifications. The quadrupole mirror ratio is 1.3, slightly higher than the value of 1.2 used in the Fokker-Planck calculations. This difference is not critical.

A view of the central flux bundle is shown in Fig. A5. Since we have not included recircularizing coils outside of the quadrupole, the flux bundle remains elliptical along the solenoidal region. The ellipticity at the mirrors is 10:1 (major to minor axis ratio). At present, we can see no objection to an elliptical flux bundle vs a cylindrical shape.

The large solenoidal magnets have a mean radius of 1.5 m, while the smaller solenoids have a radius of 0.6 m. Clear bore of the smaller coils is ~ 0.9 m, compared to the plasma column of $\sim 0.7 \times 7$ cm.

The quadrupole has a clear vertical bore of ~ 28 cm, with extended clearance in the axial direction. Our nominal beam size is 7.5×30 cm, so it appears feasible to inject several beams through a given quadrupole opening.

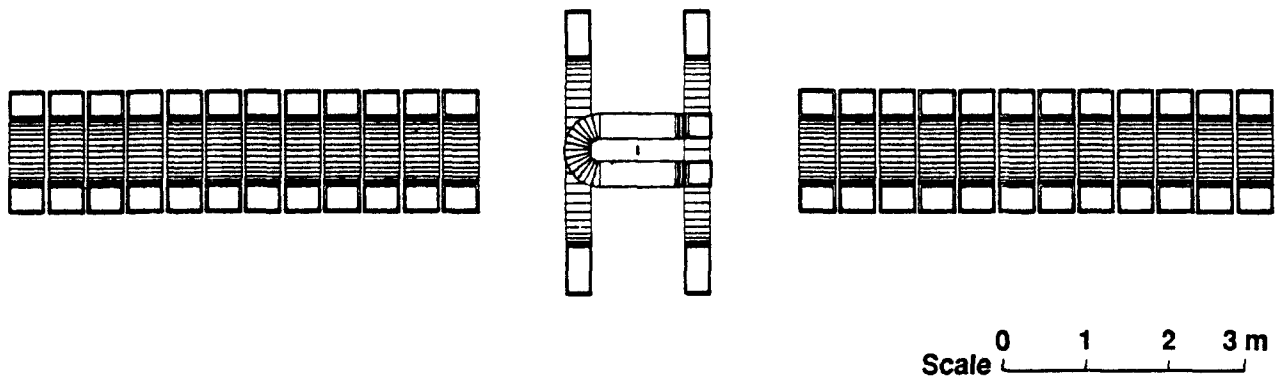


Figure A1: Magnet layout showing superconducting solenoids with center copper quadrupole insert.

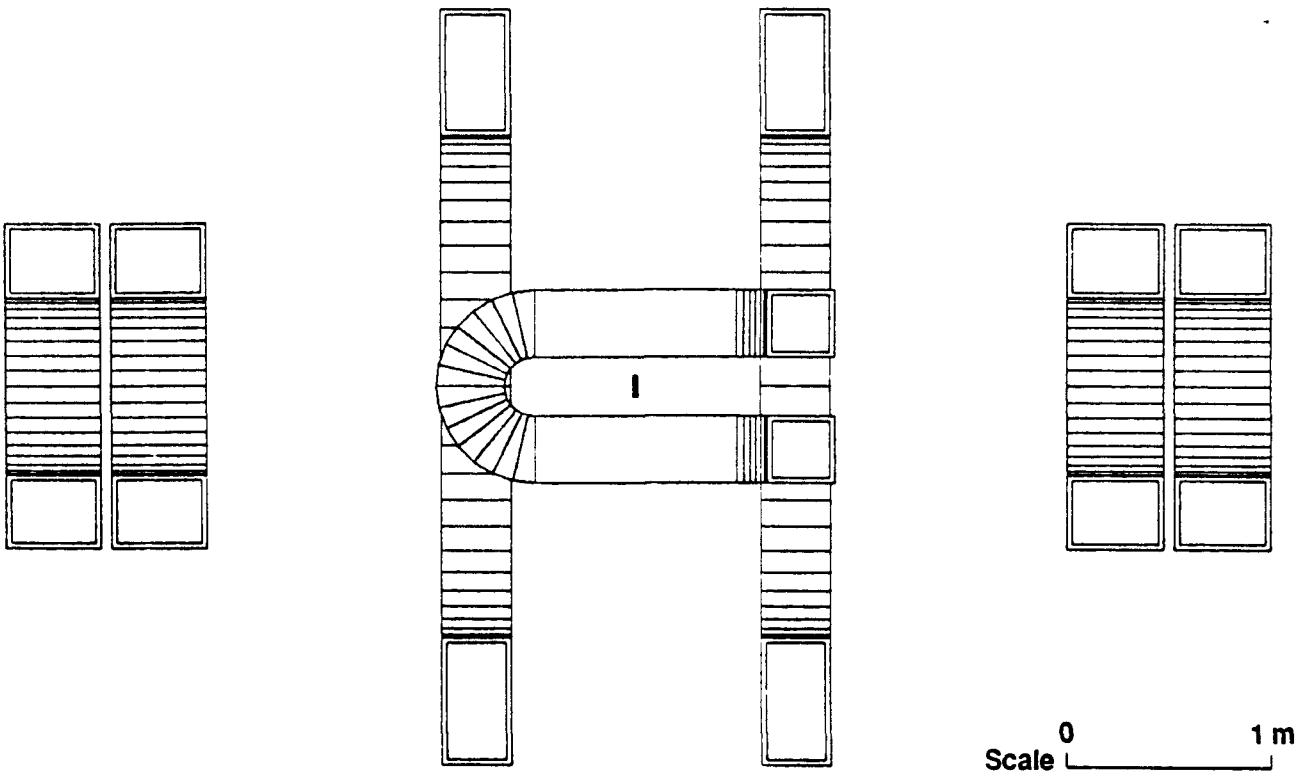
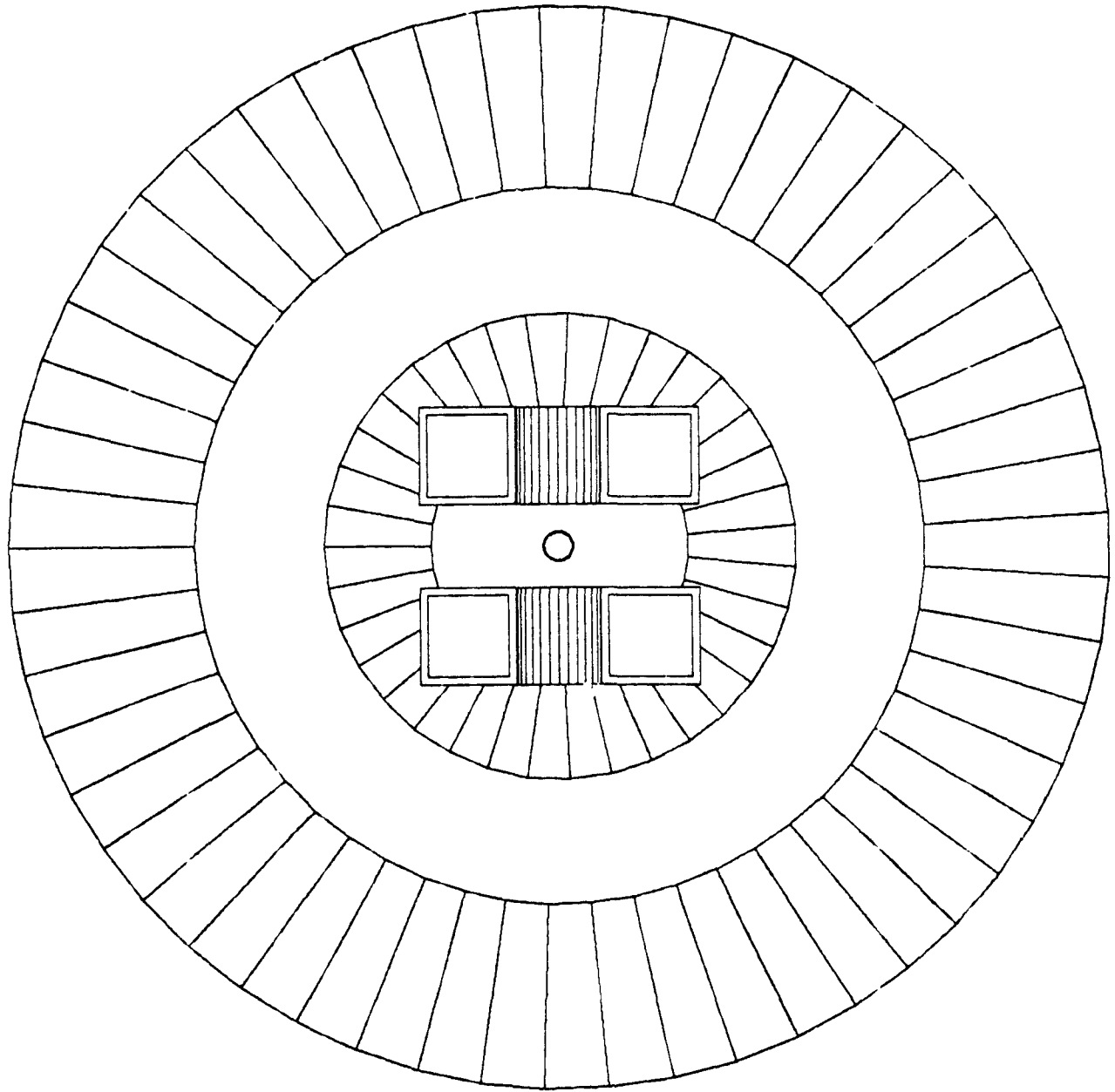


Figure A2: Enlarged view of central region.



0 1 m
Scale

Figure A3: Axial view of the central plane.

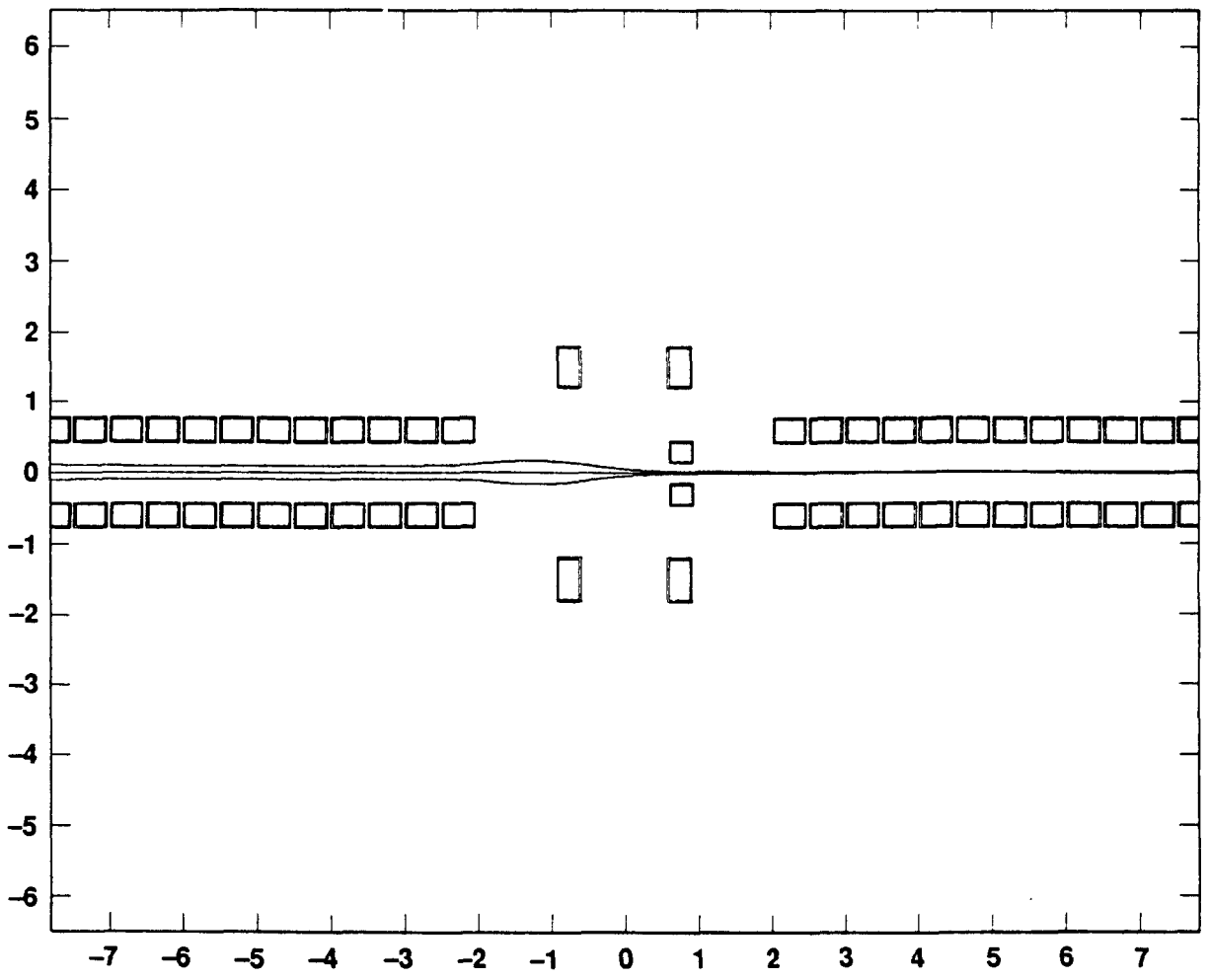


Figure A4: Axial field profile.

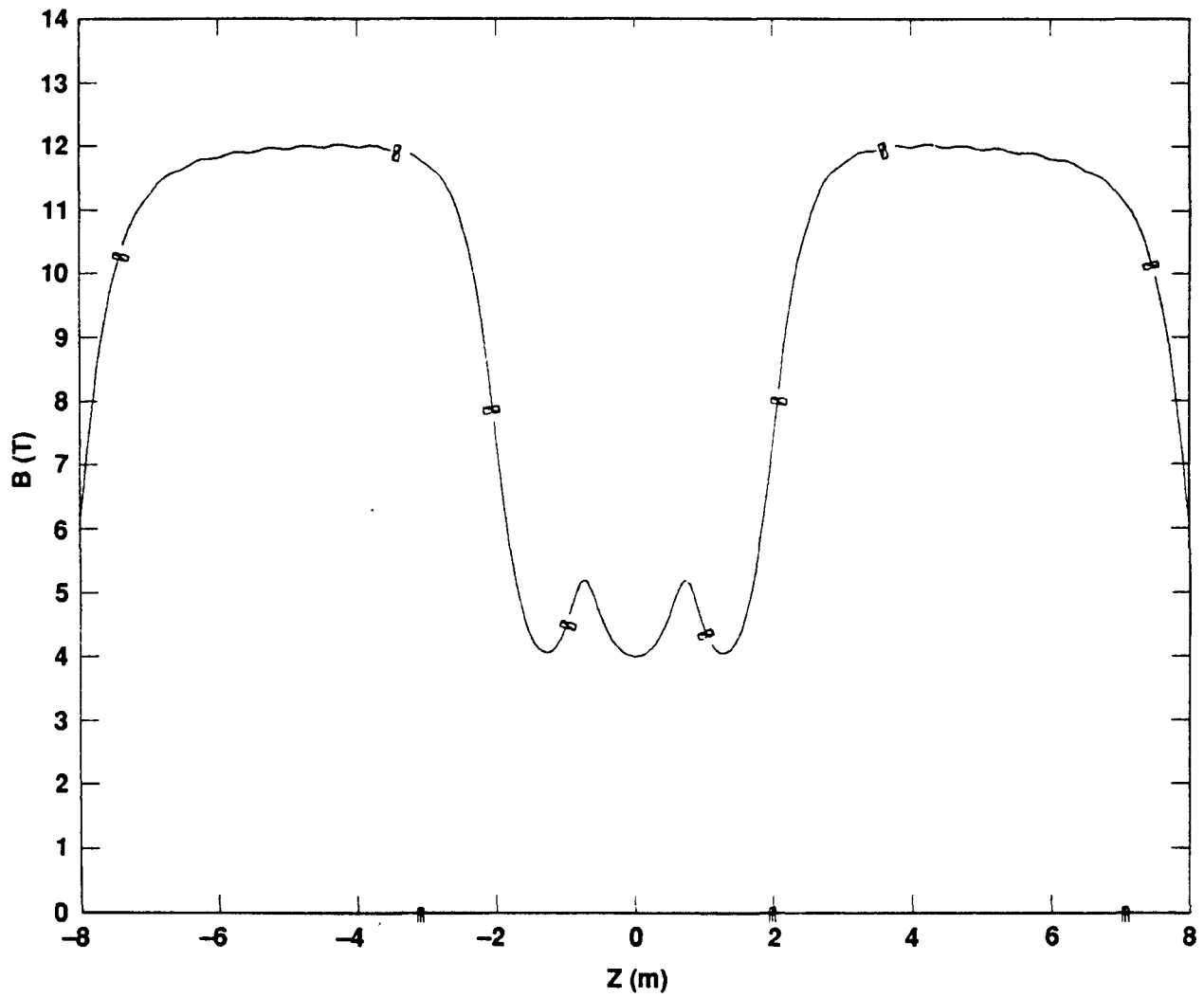


Figure A5: Flux bundle along the axis. Ellipticity at the mirror is 10.1.

We imagine two sides of the quadrupole to be used for beam injection with the other two reserved for sample probes. Detailed layouts have not yet been done.

The power required for quadrupole operation, as specified, is 6.8 MW, which seems modest and can be handled by standard water cooling (conductor packing fraction is 0.65). Trade-off studies involving beam and/or probe access and cost of operation could change the design somewhat. Also, as we better understand the MHD β -limits, we may have to alter the mirror ratio or well depth for improved stability.

The treatment of the magnetic field in the end regions has yet to be considered in detail. It may be necessary to add a magnet so as to flair the plasma into a thin fan for better interaction with the gas. This should not affect the portion of the field already specified in any way.

Acknowledgments

Work performed under the auspices of the U.S. Department of Energy by Lawrence Livermore National Laboratory under contract number W-7405-ENG-48.

References

- [1] R.F. Post, T.K. Fowler, T. Killeen, and A.A. Mirin, *Phys. Rev. Lett.* **31**, 280 (1973).
- [2] W.L. Hsu, M. Yamada, and P.J. Barrett, *Phys. Rev. Lett.* **49**, 1001 (1982).
- [3] L. Spitzer, Jr., "Physics of Fully Ionized Gases," Interscience Publishers, Inc., N.Y., 86 (1956).
- [4] T.S. Green, D.L. Fisher, A.H. Gabriel, F.T. Morgan, and A.A. Newton, *Phys. Fluids* **10**, 1663 (1967).
- [5] A.H. Futch, Jr., J.P. Holdren, J. Killeen, and A.A. Mirin, *Plasma Physics* **14** 211 (1972).
- [6] Y. Matsuda and J.J. Stewart, Jr., "A Relativistic Multiregional Bounce-Averaged Fokker-Planck Code for Mirror Plasma," Lawrence Livermore National Laboratory, UCRL-92313 (1985).

- [7] W. Heckrotte, J.R. Hiskes, and R.P. Freis, Proc. of 5th IAEA Conf. on Plasma Physics and Controlled Fusion Research, Tokyo, Japan 1974, Vol. III, p. 557, (1975). Also see "Parametric Survey for the Linear Two-Component System," Lawrence Livermore National Laboratory, UCRL-75953 Rev 1, Nov. 1974.
- [8] V.V. Mirnov *et al.*, "MHD Stability of the Gas Dynamic Trap," Preprint 84-40 (in Russian), Institute of Nuclear Physics, Novosibirsk, USSR.
- [9] FINESSE Phase 1 Report, Vol. II, p. 8-30, UCLA-ENG-85-39, Dec. 1985.
- [10] C.D. Boley, R.K. Janev, and D.E. Post, Phys. Rev. Lett., 52, 534 (1984).
- [11] D.L. Correll, "Axial Power Loss Along Open Field Lines," Lawrence Livermore National Laboratory, UCRL-96665 (1987) to be presented at Varenna, Italy, Sept. 1987.
- [12] T.D. Rognlien and T.A. Brengle, "Warm Plasma Axial Flow through a Magnetic Mirror," Phys. Fluids 24, (871) 1981.
- [13] T.D. Rognlien and T.A. Cubler, "Transition from Pastuhov to Collisional Confinement in a Magnetic and Electrostatic Well," Nuclear Fusion 20, 1003 (1980).
- [14] B.G. Logan *et al.*, Phys. Rev. Lett. 37, 1468 (1976).

Technical Information Department • Lawrence Livermore National Laboratory
University of California • Livermore, California 94550

DO NOT MICROFILM
THIS PAGE

